Vol. 42 (2011) ACTA PHYSICA POLONICA B No 5

DOORWAY STATES COUPLED TO A BACKGROUND: FIDELITY AND SURVIVAL PROBABILITY*

Thomas Guhr

Fakultät für Physik, Universität Duisburg–Essen, Duisburg, Germany

(Received April 05, 2011)

The doorway mechanism in which a distinct state is coupled to a background is encountered in a rich variety of systems. Similar scenarios are likely to be relevant in quantum information theory. We review recent analytical and numerical results obtained for various statistical observables: the distribution of the maximum overlap coefficient between doorway and the true eigenstates of the total Hamiltonian, the averaged fidelity which equals survival probability, and the distribution of fidelity.

DOI:10.5506/APhysPolB.42.1045
PACS numbers: 05.45.Mt, 03.67.–a, 24.30.Cz

1. Introduction

In more complicated quantum many-body systems, the Hilbert space is usually not organized in a "democratic" fashion, rather there are some individual states which are *distinct*, while many other states form a *background* coupled to these distinct states which can often be modelled statistically. The distinct states are then said to act as *doorways* to the background. Of course, this doorway mechanism heavily depends on how the system in question is probed. Although a recent discussion is available in Ref. [1], we briefly discuss the salient features by means of examples to make the present contribution self-contained. Consider anticrossing spectroscopy in molecular physics, see Ref. [2]. As displayed in Fig. 1, a singlet state $|s\rangle$ is excited by a laser from the singlet ground state $|s0\rangle$. This is the doorway state. It is not an eigenstate of the Hamiltonian due to a small interaction V_μ with the triplet state $|t\mu\rangle$. The interaction becomes important when the two states are energetically close. The whole manifold of triplet states forms the background. In the present case, this background can be shifted in energy by a

* Presented at the XXIII Marian Smoluchowski Symposium on Statistical Physics, "Random Matrices, Statistical Physics and Information Theory", Kraków, Poland, September 26–30, 2010.

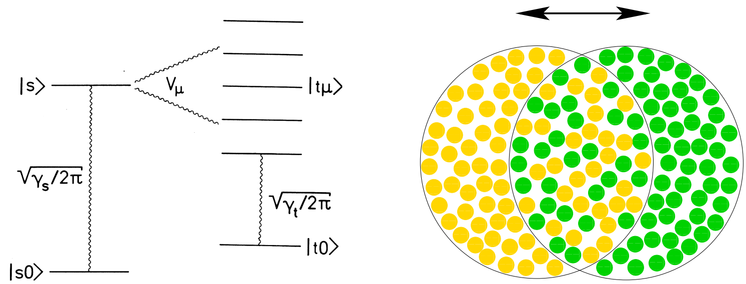

Fig. 1. Left: anticrossing spectroscopy in molecular physics, taken from Ref. [2]. Right: schematic illustration of the Giant Dipole Resonance in nuclei, taken from Ref. [1].

strong magnetic field while the singlet states, the ground state and the doorway, do not change their energetic position. Hence, whenever a triplet state is close to $|s\rangle$, the fluorescence yield from $|s\rangle$ back to $|s0\rangle$ is lowered due to the coupling V_μ. Thus, the doorway mechanism makes precise spectroscopy of the triplet levels possible.

Nuclei provide a wealth of further examples in which collective excitations are doorways. Consider the Giant Dipole Resonance [3, 4] which is found in all nuclei. The cross section of electric dipole radiation shows a huge peak at higher excitation energies which can be interpreted in a schematic, semiclassical picture according to Fig. 1. Ignoring the relative motion of protons to one another and neutrons to one another, we view the nucleons as confined in two spheres, one for the protons, one for the neutrons, within which the particles are "frozen". The excitation is then the one-dimensional linear oscillation of these two spheres against each other. In this schematic picture, the excitation is fully collective, *i.e.* coherent in phase space. The corresponding state, however, is certainly not an eigenstate of the true many-body Hamiltonian. A true eigenstate must contain contributions due to the relative motion of the particles within each sphere. It becomes more relevant the further the excitation energy is away from the peak energy. A broad resonance results with a typical spreading width Γ. It measures the coupling strength between the schematic model for the collective state and the surrounding background states which are of single-particle type. The true states are thus superpositions. The local density of states around the peak has a Lorentzian shape and is referred to as Breit–Wigner line. It is very robust [3].

The doorway mechanism has been identified in numerous systems, metal clusters are another example, see Refs. [5, 6]. In quantum chaos [7], yet another example for the doorway mechanism was recently investigated in Ref. [8]. The distinct states are superscars in a pseudo integrable microwave billiard which exist together with a large number of non-scarring states forming the background. In contrast to the previous examples, the wave functions could be measured, rendering a full-fledged statistical study possible which can, at least nowadays, not be carried out in many-body systems. In this context, the distribution of the coupling coefficients is of high interest. Here, we will review recent analytical results [9] for the case of different statistical choices for the background.

The doorway mechanism turns out to be relevant in the quickly expanding field of quantum information. Here, one wishes to know how well a prepared state can be isolated and how the unavoidable mixing with the surrounding behaves. Of course, different ways are conceivable in which the prepared states and the states forming the surrounding are coupled. One possible way is certainly the one which maps one-to-one to the doorway mechanism: a prepared state is identified with a doorway, the surrounding with the background, and the mixing with the coupling. The interesting objects here are the fidelity averaged over the background which coincides with the survival probability. We review recent analytical and numerical results obtained in Refs. [10, 11].

The paper is organized as follows. In Sec. 2, the doorway mechanism is modelled and statistical assumptions are discussed. The distribution of the maximum overlap coefficients is studied in Sec 3. In Sec. 4, fidelity, survival probability and their distribution are addressed. We summarize in Sec. 5.

2. Modelling the doorway mechanism

For the convenience of the reader, we sketch the statistical model of the doorway mechanism, see also Refs. [3, 8]. The total Hamiltonian

$$\hat{H} \;=\; \hat{H}_{\mathrm{S}} + \hat{H}_{\mathrm{B}} + \hat{V} \tag{2.1}$$

has three parts: $\hat{H}_{\mathrm{S}}$ and $\hat{H}_{\mathrm{B}}$ are the Hamiltonians for doorway and background states, respectively. The interaction $\hat{V}$ couples these two classes of states. The Schrödinger equations for the doorway and background Hamiltonians are

$$\hat{H}_{\mathrm{S}}|s\rangle = E_s|s\rangle \qquad \text{and} \qquad \hat{H}_{\mathrm{B}}|b\rangle = E_b|b\rangle\,. \tag{2.2}$$

One assumes that the interaction only couples states from different classes,

$$\langle s|\hat{V}|s'\rangle = \langle b|\hat{V}|b'\rangle = 0 \qquad \text{and} \qquad \langle b|\hat{V}|s\rangle = V_{bs} \tag{2.3}$$

for any s, s', b, b'. As already pointed out in Sec. 1, a doorway state is not an eigenstate of the Hamiltonian $\hat{H}$. For the sequel, we may assume that there is only one doorway state $|s\rangle$. The Schrödinger equation for the full Hamiltonian,

$$\hat{H}|n\rangle = \mathcal{E}_n|n\rangle \tag{2.4}$$

can be solved, the exact but implicit equation

$$\mathcal{E}_n = E_s - \sum_{b=1}^{N} \frac{V_{bs}^2}{E_b - \mathcal{E}_n} \tag{2.5}$$

results. The *true* eigenstates are found to be

$$|n\rangle = c_{sn}\left(|s\rangle - \sum_{b=1}^{N} \frac{V_{bs}}{E_b - \mathcal{E}_n}|b\rangle\right) . \tag{2.6}$$

Employing the normalization, one finds the formula

$$c_{sn} = \langle n|s\rangle = \left(1 + \sum_{b=1}^{N} \frac{V_{bs}^2}{(E_b - \mathcal{E}_n)^2}\right)^{-1/2} \tag{2.7}$$

for the overlap coefficients of the doorway $|s\rangle$ to each true eigenstate $|n\rangle$.

So far, statistical assumptions have not been made. To introduce such, we now go over to a matrix description by writing

$$H = \begin{bmatrix} E_s & V^\dagger \\ V & H_\mathrm{B} \end{bmatrix} , \tag{2.8}$$

where E_s is the energy of the doorway and where the background matrix H_B has dimension $N \times N$. We model H_B by random matrices over which an ensemble average is taken. A review of Random Matrix Theory can be found in Ref. [12]. To obtain meaningful results, the cut-off N has to be sent to infinity at the end of all calculations. It is a well-known general result of Random Matrix Theory that all statistical observables then depend only on $\langle V^2\rangle = V^\dagger V/N$. This quantity has to be compared with the mean level spacing D of the background states such that

$$\lambda = \frac{\sqrt{\langle V^2\rangle}}{D} \tag{2.9}$$

turns out to be the proper dimensionless parameter measuring the average coupling strength to the doorway. The above mentioned width of the Breit–Wigner line is in this model given by $\Gamma = 2\pi\langle V^2\rangle/D = 2\pi\lambda^2 D$. These statements apply even without making statistical assumptions about the interaction matrix elements V_{bs}, but usually one takes them as Gaussian distributed random variables centred around zero with variance v^2 which then replaces $\langle V^2\rangle$.

3. Distribution of the maximum overlap coefficients

In Ref. [8], the maximum overlap coefficient, more precisely its maximum modulus,

$$c_{\max} = \max\left(|c_{sn}|\right) \tag{3.1}$$

was found to be a useful quantity because its distribution

$$p_{\max}(c) = \langle \delta(c - c_{\max}) \rangle_{H_{\mathrm{B}},V} \tag{3.2}$$

depends very sensitively on the average coupling strength and thus allows for a reliable extraction of the parameter λ. This was demonstrated for the data obtained in the experiment. The empirical distributions were also shown to compared well with random matrix simulations. In Ref. [9], we derived analytical results for the case of weak coupling λ. Then, the overlap c_{s0} between the *unperturbed* doorway state $|s\rangle$ (at $\lambda = 0$) and the *evolved* doorway state $|0\rangle$ (at $\lambda > 0$) should be largest. Thus, we approximately have

$$p_{\max}(c) \;\approx\; p_0(c) = \langle \delta(c - |c_{s0}|) \rangle_{H_{\mathrm{B}},V} \,. \tag{3.3}$$

We managed to calculate the distribution $p_0(c)$ analytically and found closed form results [9]. In the case of a regular background, *i.e.*, Poisson statistics for H_{B}, the calculation is rather straightforward. We found

$$p_0^{\mathrm{Poisson}}(c) = \frac{2a_\beta\lambda}{(1-c^2)^{3/2}} \exp\left(-\,(a_\beta\lambda)^2 \,\frac{\pi c^2}{1-c^2} \right) \tag{3.4}$$

for arbitrary, factorizing distributions of the coupling matrix elements V_{bs}. We distinguished real and complex coupling, labelled $\beta = 1$ and $\beta = 2$, respectively. The numerical values for the parameters a_β differ for the chosen distributions of the coupling matrix elements. In the Gaussian case, we found the values

$$a_\beta \;=\; \begin{cases} \sqrt{2/\pi} & \approx \quad 0.80\,, \qquad \beta = 1\,, \\ \sqrt{\pi/4} & \approx \quad 0.89\,, \qquad \beta = 2\,, \end{cases} \tag{3.5}$$

which are numerically very similar.

For a chaotic background, we studied real symmetric and Hermitean matrices H_{B}, *i.e.*, we drew them either from the Gaussian Orthogonal Ensemble (GOE) or from the Gaussian Unitary Ensemble (GUE). The symmetries of the total Hamiltonian then require that the coupling matrix elements V_{bs} are real in the GOE and complex in the GUE case. Furthermore, it follows from general considerations that the choice of distribution for the coupling matrix elements is largely irrelevant in such chaotic cases [12]. We thus settled with Gaussian distributions. To proceed, we had to resort to the supersymmetry method. The rather complicated calculations will not be presented here.

Luckily, the results for different choices for the statistics of the background matrix $H_{\rm B}$ are quite compact. We obtained

$$
\begin{aligned}
p_0^{\rm GOE}(c) &= \sqrt{\frac{\pi^3\lambda^6c^4}{2(1-c^2)^5}}\exp\left(-\frac{\pi^2\lambda^2c^2}{4(1-c^2)}\right) \\
&\quad\times\left(K_0\left(\frac{\pi^2\lambda^2c^2}{4(1-c^2)}\right)+K_1\left(\frac{\pi^2\lambda^2c^2}{4(1-c^2)}\right)\right), \\
p_0^{\rm GUE}(c) &= \sqrt{\frac{\pi\lambda^2}{(1-c^2)^3}}\exp\left(-\frac{\pi^2\lambda^2c^2}{(1-c^2)}\right)\left(1+\frac{2\pi^2\lambda^2c^2}{1-c^2}\right). \qquad (3.6)
\end{aligned}
$$

As often, the GOE result is the more complicated one, it contains the modified Bessel functions K_0 and K_1 of the second kind.

As seen in Fig. 2, the distributions sensitively depend on the coupling strength λ. For $\lambda = 0.1$, most overlap coefficients are very small, and the few which are not are close to unity. For $\lambda = 2.0$, however, the doorway spreads over the entire background spectrum, and many coefficients have smaller and only very few have larger values. An intermediate situation is found for $\lambda = 0.5$. Our weak coupling approximation (3.3) is valid for $\lambda = 0.1$ and $\lambda = 0.5$, but even for $\lambda = 2.0$ it gives qualitatively the right picture for $p_{\rm max}(c)$. Importantly, the results for a given λ are not very different for regular and chaotic background, and in the chaotic case not very different for real and Hermitean symmetry. Hence, a reliable extraction of the coupling strength λ is possible, even if one has little or no information about the statistics of the background states.

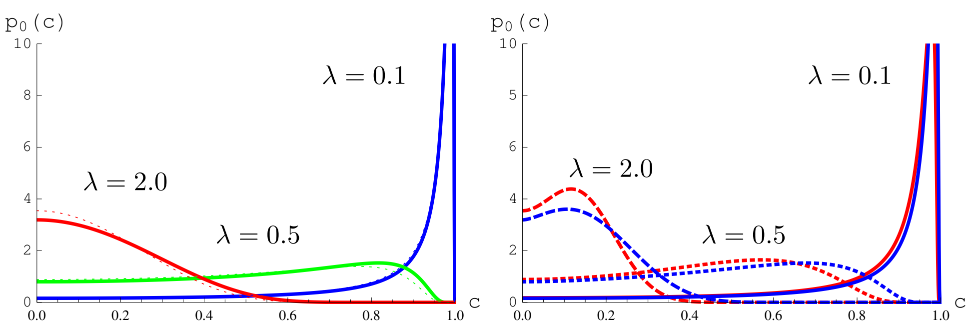

Fig. 2. Distribution $p_0(c)$, analytical results for three different values of the coupling parameter λ, adopted from Ref. [9]. Left: regular background, real (solid line) and complex (thin dashed line) coupling matrix elements. Right: chaotic background, for a given λ, the GUE result is slightly shifted to the left as compared to the GOE result.

4. Fidelity, survival probability and their distribution

We turn to the observables which are of interest in quantum information. In the sequel, we compile the main points of the discussion in Refs. [10, 11]. The fidelity amplitude $f(t)$ is the overlap between the time evolved states

$$\exp\left(-\frac{i}{\hbar}\left(\hat{H}_{\rm S}+\hat{H}_{\rm B}\right)t\right)|s\rangle \quad \text{and} \quad \exp\left(-\frac{i}{\hbar}\left(\hat{H}_{\rm S}+\hat{H}_{\rm B}+\hat{V}\right)t\right)|s\rangle\,. \tag{4.1}$$

Without loss of generality, we may choose $E_s = 0$ for the doorway energy. We then easily find

$$f(t) = \langle s|\exp\left(-\frac{i}{\hbar}\hat{H}t\right)|s\rangle = \sum_n |c_{sn}|^2 \exp\left(-\frac{i}{\hbar}\mathcal{E}_n t\right)\,, \tag{4.2}$$

where $\hat{H} = \hat{H}_{\rm S}+\hat{H}_{\rm B}+\hat{V}$ is the total Hamiltonian. The Fourier transform

$$\rho(E) = \sum_n |c_{sn}|^2 \delta(E-\mathcal{E}_n) \tag{4.3}$$

is the local density of states which has, as mentioned in Sec. 1, a Lorentzian shape under very general conditions on the background and the coupling matrix elements. The fidelity is given by

$$F(t) = |f(t)|^2\,. \tag{4.4}$$

We decompose it into a diagonal and an off-diagonal part,

$$F(t) = \sum_{m,n} |c_{sm}|^2|c_{sn}|^2 \exp\left(\frac{i}{\hbar}(\mathcal{E}_m-\mathcal{E}_n)t\right) = \text{IPR} + F_{\rm fluc}(t)\,. \tag{4.5}$$

The diagonal part

$$\text{IPR} = \sum_n |c_{sn}|^4 \tag{4.6}$$

is in solid state physics referred to as "inverse" participation ratio. It is time independent, while the off-diagonal part

$$F_{\rm fluc}(t) = 2\sum_{m\neq n} |c_{sm}|^2|c_{sn}|^2 \cos\left(\frac{\mathcal{E}_m-\mathcal{E}_n}{\hbar}\,t\right) \tag{4.7}$$

strongly fluctuates with time. The survival probability

$$P(t) = \langle F(t)\rangle_{H_{\rm B},V} \tag{4.8}$$

is in the present context simply the averaged fidelity.

Of course, at first sight, one expects the survival probability to decay as time grows. A "Drude approximation" seems to support that. If we replace the average of the modulus squared with the modulus squared of the average,

$$P(t) = \langle F(t)\rangle_{H_{\rm B},V} = \left\langle |f(t)|^2\right\rangle_{H_{\rm B},V} \approx |\langle f(t)\rangle_{H_{\rm B},V}|^2 = \exp(-\Gamma t)\,, \qquad (4.9)$$

we arrive at an exponential decay because we know that the local density of states (4.3) has Lorentzian shape with width Γ. This decay can be viewed as due to Fermi's Golden Rule. However, the first correction to be added is the average inverse participation ratio $\langle \mathrm{IPR}\rangle_{H_{\rm B},V} = D/\pi\Gamma$ which remains constant in the limit $t \to \infty$. But this cannot be the final answer yet, because $\langle \mathrm{IPR}\rangle_{H_{\rm B},V}$ has an unphysical divergence for $\Gamma = 0$, *i.e.*, $\lambda = 0$. Gruver *et al.* [13] assumed random matrix statistics for the background states and calculated further corrections. Their final result is approximative, but it shows a revival of the survival probability at larger times. The saturation value is coupling dependent and given by the average inverse participation ratio, $P(\infty) = \langle \mathrm{IPR}\rangle_{H_{\rm B},V}$.

Using supersymmetry, the survival probability was calculated exactly in Refs. [10, 11] for complex coupling. The rather involved details will not be presented here. For a technical reason, the case of real coupling remained analytically inaccessible, but was simulated numerically. The results are shown in Fig. 3 *versus* time in units of the Heisenberg time. The revival and the saturation are clearly seen. Once more, we observe that the type of coupling, *i.e.*, real or complex, is more significant than the type of background statistics, where real and Hermitean symmetry yield almost the same curves in the chaotic case while the curve for the regular case is a bit above. Wu *et al.* [14] experimentally studied a system which can be interpreted as a doorway coupled to a background. They realized a quantum kicked rotor by atomic interferometry of matter waves in a periodically pulsed optical standing wave. Although the details of the setup are difficult to understand, we are quite confident that they indeed measure the survival probability *versus* time. The curves are very similar to the ones in Fig. 3.

Finally, we address the distribution

$$Q_t(z) = \langle \delta(z - F(t))\rangle_{H_{\rm B},V} \qquad (4.10)$$

of the fidelity which parametrically depends on time. At least for now, we do not know how to calculate this quantity analytically, but we carried out detailed numerical simulations in Ref. [10]. In Fig. 4, results are displayed for real coupling matrix elements with strength $\lambda = 0.1$ and a GOE background. For $t = 1$, the distribution is very sharp, it becomes broader for larger times and reaches a stable limit for $t > 20$. This is so, because the contribution of the fluctuating part (4.7) must be exhausted beyond a certain time scale.

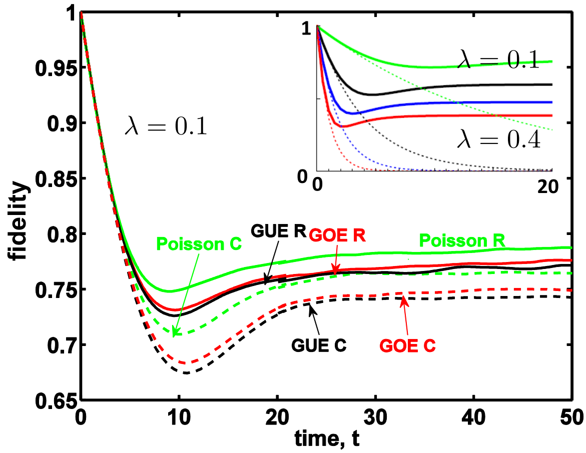

Fig. 3. Average fidelity $P(t)$ which equals survival probability, adopted from [10]. Curves in the main figure are for coupling strength $\lambda = 0.1$. The full lines correspond top down to real coupling to a Poisson, to a GOE and to a GUE background. The dashed lines describe top down complex coupling to the same backgrounds. The inset shows the survival probability on shorter times top down for $\lambda = 0.1$, 0.2, 0.3 and 0.4 for complex coupling to Poisson background. For comparison, the exponential decay is shown as thinner dotted lines.

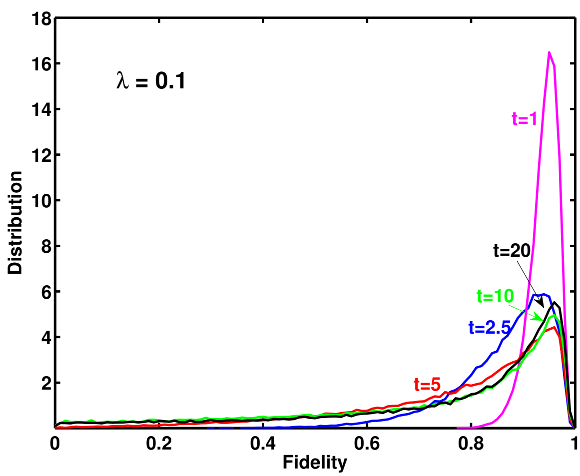

Fig. 4. Fidelity distribution $Q_t(z)$ for real coupling matrix elements with strength $\lambda = 0.1$ and a GOE background, taken from Ref. [10]. The curves correspond to times $t = 1$, $t = 2.5$, $t = 5$, $t = 10$ and $t = 20$. For times $t > 20$ the distribution is stable.

In Fig. 5, we compare three distributions for real coupling matrix elements with strength $\lambda = 0.05$ and a GOE background. The distribution of fidelity in the stable limit must have a finite contribution due to the fluctuating part (4.7). Hence, as to be expected, it is sharper and has a higher peak than the distribution of the inverse participation ratio (4.6). The latter is seen to be indistinguishable form the distribution of the maximum overlap coefficient to the fourth power which can easily be obtained from the results given in Sec. 3. For the very weak coupling strength $\lambda = 0.05$ this ought to be so, because the inverse participation ratio is dominated by the contribution from the overlap coefficient c_{s0}.

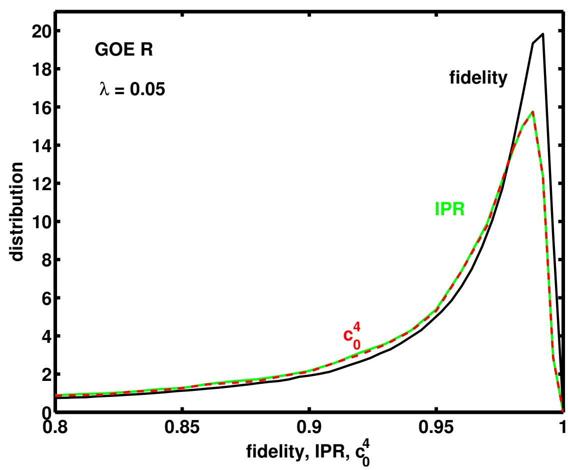

Fig. 5. Comparison of three distributions for real coupling matrix elements with strength $\lambda = 0.05$ and a GOE background, taken from Ref. [10]. The distribution of fidelity in the stable limit peaks highest. The distribution of the inverse participation ratio IPR and of the maximum overlap coefficient to the fourth power, here denoted c_0^4, peak lower and are indistinguishable.

5. Summary

The doorway mechanism is ubiquitous in physics, it is found in numerous many-body and other systems, particularly in quantum chaotic ones. The doorways are somehow distinct, for example due to a simple semiclassical or schematic interpretation. They are coupled to a background of states which in our context can be treated statistically. Prompted by recent experimental studies, we analytically calculated the distribution of the maximum overlap coefficient between doorway and the true eigenstates of the total Hamiltonian. We did that in the framework of a random matrix model for weak coupling.

In quantum information theory, one is interested in isolating prepared states, *i.e.*, one needs to know how the mixing to the surrounding influences these prepared states as time evolves. One possible scenario can be mapped one-to-one to the doorway mechanism. The relevant statistical observables are then the averaged fidelity which equals survival probability. Exact analytical calculations as well as numerical simulations confirm and extend earlier approximative results which yield an exponential decay followed by a revival and a finite saturation limit. There is a striking difference for real and complex couplings. The distribution of fidelity has a stable limit beyond a certain time scale.

I thank my collaborators Sven Åberg, Heiner Kohler and Hans-Jürgen Sommers. I acknowledge support from Deutsche Forschungsgemeinschaft within the Transregional Collaborative Research Center SFB/TR12 "Symmetries and Universality in Mesoscopic Systems".

REFERENCES

[1] T. Guhr, *Acta Phys. Pol. A* **116**, 741 (2009).

[2] T. Guhr, H.A. Weidenmüller, *Chem. Phys.* **146**, 21 (1990).

[3] A. Bohr, B. Mottelson, *Nuclear Structure* Vol. 1, ed. W.A. Benjamin INC, 1969.

[4] V. Zelevinsky, *Annu. Rev. Nucl. Part. Sci.* **46**, 237 (1996).

[5] I. Kawata, H. Kono, Y. Fujimura, A.D. Bandrauk, *Phys. Rev.* **A62**, 031401(R) (2000).

[6] M.S. Hussein, V. Kharchenko, L.F. Canto, R. Donangelo, *Ann. Phys.* **284**, 178 (2000).

[7] H.-J. Stöckmann, *Quantum Chaos: An Introduction*, Cambridge University Press, Cambridge 2000.

[8] S. Åberg, T. Guhr, M. Miski-Oglu, A. Richter, *Phys. Rev. Lett.* **100**, 204101 (2008).

[9] H. Kohler, T. Guhr, S. Åberg, *New J. Phys.* **12**, 073026 (2010).

[10] H. Kohler, H.-J. Sommers, S. Åberg, T. Guhr, *Phys. Rev.* **E81**, 050103(R) (2010).

[11] H. Kohler, H.-J. Sommers, S. Åberg, *J. Phys. A: Math. Theor.* **43**, 215102 (2010).

[12] T. Guhr, A. Müller-Groeling, H.A. Weidenmüller, *Phys. Rep.* **299**, 189 (1998).

[13] J.L. Gruver *et al.*, *Phys. Rev.* **E55**, 6370 (1997).

[14] S. Wu, A. Tonyushki, M.G. Prentiss, *Phys. Rev. Lett.* **103**, 034101 (2009).